

Basic Study

Structural and molecular features of intestinal strictures in rats with Crohn's-like disease

Petra Talapka, Anikó Berkó, Lajos István Nagy, Lalitha Chandrakumar, Mária Bagyánszki, László Géza Puskás, Éva Fekete, Nikolett Bódi

Petra Talapka, Anikó Berkó, Lalitha Chandrakumar, Mária Bagyánszki, Éva Fekete, Nikolett Bódi, Department of Physiology, Anatomy and Neuroscience, Faculty of Sciences and Informatics, University of Szeged, H-6726 Szeged, Hungary

Lajos István Nagy, László Géza Puskás, Avidin Ltd., H-6726 Szeged, Hungary

Author contributions: Talapka P and Berkó A contributed equally to this work; Talapka P performed the majority of experiments and analyzed the data; Berkó A and Nagy LI performed the molecular investigations; Chandrakumar L and Bódi N participated equally in treatment of animals; Bagyánszki M, Puskás LG, Fekete E and Bódi N designed and coordinated the research; Talapka P, Fekete E and Bódi N wrote the paper; Talapka P and Berkó A contributed equally to this work.

Supported by Hungarian Scientific Research Fund, No. OTKA PD 108309 to Bódi N; and the János Bolyai Research Scholarship of the Hungarian Academy of Sciences to Bagyánszki M.

Institutional review board statement: The study was reviewed and approved by the Institutional Review Board of the Department of Anatomy, Physiology and Neuroscience, Faculty of Sciences, University of Szeged.

Institutional animal care and use committee statement: All procedures involving animals were reviewed and approved by the Institutional Animal Care and use committee of the University of Szeged (protocol number: EIK-645/2014.02.05).

Conflict-of-interest statement: We certify that there is no actual or potential conflict of interest in relation to this article.

Data sharing statement: Technical appendix, statistical code, and dataset available from the corresponding author, Mária Bagyánszki at bmarcsi@bio.u-szeged.hu.

Open-Access: This article is an open-access article which was selected by an in-house editor and fully peer-reviewed by external reviewers. It is distributed in accordance with the Creative Commons Attribution Non Commercial (CC BY-NC 4.0) license,

which permits others to distribute, remix, adapt, build upon this work non-commercially, and license their derivative works on different terms, provided the original work is properly cited and the use is non-commercial. See: <http://creativecommons.org/licenses/by-nc/4.0/>

Correspondence to: Mária Bagyánszki, PhD, Associate Professor, Department of Physiology, Anatomy and Neuroscience, Faculty of Sciences and Informatics, University of Szeged, H-6726 Szeged, Közép fasor 52, Hungary. bmarcsi@bio.u-szeged.hu
Telephone: +36-62-544123
Fax: +36-62-544291

Received: February 2, 2016
Peer-review started: February 9, 2016
First decision: March 7, 2016
Revised: March 23, 2016
Accepted: April 7, 2016
Article in press: April 7, 2016
Published online: June 14, 2016

Abstract

AIM: To develop a new rat model we wanted to gain a better understanding of stricture formation in Crohn's disease (CD).

METHODS: Chronic colitis was induced locally by the administration of 2,4,6-trinitrobenzenesulfonic acid (TNBS). The relapsing inflammation characteristic to CD was mimicked by repeated TNBS treatments. Animals were randomly divided into control, once, twice and three times TNBS-treated groups. Control animals received an enema of saline. Tissue samples were taken from the strictured colonic segments and also adjacent proximally and distally to its 60, 90 or 120 d after the last TNBS or saline administrations. The frequency and macroscopic extent of the strictures were measured on digital photographs. The structural

features of strictured gut wall were studied by light- and electron microscopy. Inflammation related alterations in TGF-beta 2 and 3, matrix metalloproteinases 9 (MMP9) and TIMP1 mRNA and protein expression were determined by quantitative real-time PCR and western blot analysis. The quantitative distribution of caspase 9 was determined by post-embedding immunohistochemistry.

RESULTS: Intestinal strictures first appeared 60 d after TNBS treatments and the frequency of them increased up to day 120. From day 90 an intact lamina epithelialis, reversible thickening of lamina muscularis mucosae and irreversible thickening of the muscularis externa were demonstrated in the strictured colonic segments. Nevertheless the morphological signs of apoptosis were frequently seen and excess extracellular matrix deposition was recorded between smooth muscle cells (SMCs). Enhanced caspase 9 expression on day 90 in the SMCs and on day 120 also in myenteric neurons indicated the induction of apoptosis. The mRNA expression profile of TGF-betas after repeated TNBS doses was characteristic to CD, TGF-beta 2, but not TGF-beta 3 was up-regulated. Overexpression of MMP9 and down-regulation of TIMP1 were demonstrated. The progressive increase in the amount of MMP9 protein in the strictures was also obvious between days 90 and 120 but TIMP1 protein was practically undetectable at this time.

CONCLUSION: These findings indicate that aligned structural and molecular changes in the gut wall rather than neuronal cell death play the primary role in stricture formation.

Key words: Crohn's disease; Rat model; TGF-beta; Intestinal strictures; MMP9; TIMP1

© **The Author(s) 2016.** Published by Baishideng Publishing Group Inc. All rights reserved.

Core tip: Intestinal strictures in Crohn's disease (CD) cause hardly treatable complications in patients. The aim of this study was to find the correlation between the intestinal stricture formation, the damaged innervation of smooth muscle cells (SMCs) and the changed expression of TGF-beta 2, 3 and MMP9/TIMP1 in rats with CD by using different light- and electron microscopic and molecular biological methods. Our findings indicate that disintegration of SMCs due to the up-regulation of TGF-beta 2 and off-balance in MMP9/TIMP1 expression rather than neuronal cell death play the primary role in the formation of intestinal strictures in CD.

Talapka P, Berkó A, Nagy LI, Chandrakumar L, Bagyánszki M, Puskás LG, Fekete E, Bódi N. Structural and molecular features of intestinal strictures in rats with Crohn's-like disease. *World J Gastroenterol* 2016; 22(22): 5154-5164 Available from: URL: <http://www.wjgnet.com/1007-9327/full/v22/i22/5154.htm> DOI: <http://dx.doi.org/10.3748/wjg.v22.i22.5154>

INTRODUCTION

Despite the fact that the formation of obstructive strictures is the leading cause of surgical intervention in patients with Crohn's disease (CD), little is known about their etiopathogenesis, and no direct therapies are available for the effective prevention or reversal of this condition^[1]. Lasting deep remission has emerged as a major therapeutic goal in CD^[2,3]. This implies not only alleviation of the symptoms, but also the achievement of complete mucosal healing, with the accompanying decrease in the risk of irreversible pathological alterations of the gut wall^[4]. However, total mucosal regeneration to prevent stricture formation is unattainable^[5,6].

The spread of fibrosis deep into the gut wall leads to disorganization of the lamina muscularis mucosae (LMM) and thickening of all layers of the gut wall due to the accumulation of extracellular matrix (ECM) elements^[5,6]. Previous studies have demonstrated that the cytokines transforming growth factor-beta (TGF- β) isoforms and the tissue-degrading matrix metalloproteinases (MMPs) are the key contributors to these processes^[7,8]. Both TGF-beta and its receptors are overexpressed in the intestine of CD patients. However, the expression of the TGF-beta isoforms varies with the nature of the tissue. Fibrotic tissue exhibits a reduced expression of TGF-beta 3 and an enhanced expression of TGF-beta 2^[9-11]. MMPs are secreted as inactive zymogens which must undergo proteolytic cleavage to become active, and their activity is regulated by specific tissue inhibitors of metalloproteinases (TIMPs)^[12-14]. The MMPs do not simply degrade ECM as their name might suggest, but are also responsible for the homeostatic regulation of the ECM. Previous studies have shown that the gene transcription of MMP9 is inducible and that the promoter region is highly responsive to most growth factors and cytokines. They directly cleave and activate growth factors into active ligands, and therefore regulate their bioavailability and/or activity^[15-17]. In consequence of these complex interactions of the regulatory processes, the development of the intestinal strictures characteristic of CD cannot be explained simply by the lower or higher expression of one or other of these factors. The key driver of stricture formation rather appears to be an off-balance between the TGF-betas, MMPs and TIMPs which develops in the chronic phase of inflammation. MMP9 is the most abundant MMP expressed in colonic tissue from CD patients, and may therefore be regarded as a biomarker in the evaluation of the clinical activity of inflammatory bowel diseases (IBDs)^[18].

The intestinal symptoms common among CD patients are often related to enteric neuropathy. The evidence suggests that both the quantitative properties and function of the myenteric neurons are altered substantially by intestinal inflammation^[19-22] and in fact complete loss of the myenteric neurons has been

observed in the strictured regions^[23]. However, the extent to which the deficient innervation of the smooth muscle cells (SMCs) and/or the imbalance in the regulation in the molecular events behind the tissue remodelling are responsible for the stricture formation remains unclear.

We recently reported on a rat model of chronic colitis where the mortality was negligible despite the severity of the intestinal symptoms. We demonstrated that experimentally provoked recurring periods of acute inflammation exerted a preconditioning effect against the mucosal damage and reduced the rapid, significant and widespread loss of myenteric neurons observed after the induction of the colitis^[24]. In the present work, we used this model to investigate the long-term consequences of acute inflammation on the structural and molecular alterations in the strictured gut wall. The aim of the study was to investigate the possible coincidence between the expressions of TGF- β s, MMP9 and TIMP1 behind the structural remodelling of the strictured gut wall. The structural findings at the light- and electron microscopic levels and the molecular findings at the mRNA and protein levels will be discussed.

MATERIALS AND METHODS

Animal model

All procedures involving experimental animals were approved from the Local Ethics Committee for Animal Research Studies at the University of Szeged. Adult male Sprague-Dawley rats weighing 200-220 g were used throughout the experiments. The animal protocol was designed to minimize pain or discomfort to the animals. The rats were acclimatized to laboratory conditions (23 °C, 12 h/12 h light/dark, 50% humidity, *ad libitum* access to food and water) for two weeks prior to experimentation. Colitis was induced locally under pentobarbital anaesthesia (45 mg/kg *ip*) by the administration of 2,4,6-trinitrobenzenesulfonic acid (TNBS; Sigma-Aldrich, St. Louis, MO, United States; 10 mg) dissolved in 0.25 mL of 25% ethanol, as described earlier^[24]. Repetitive relapsing inflammation (RRI) was mimicked through repeated administration of the same TNBS doses. The rats were treated once ($n = 8$), twice ($n = 7$) or three times ($n = 8$) with TNBS, 2 weeks passed between the treatments. Control rats ($n = 18$) received an enema of 0.25 mL of 9 g/L saline at the same time as the TNBS was administered. The rats were weighed and monitored daily for activity, bloody diarrhoea and mortality and were sacrificed 60, 90 or 120 d after the last TNBS or saline administrations.

Tissue handling

The animals were killed by cervical dislocation under pentobarbital anaesthesia. After this the last 8 cm region of the descending colon from the anus was dissected. Digital photographs were taken to

evaluate the frequency and macroscopic extent of the strictures. Three colonic tissue samples were taken from each animal: the stricture itself and samples adjacent proximally and distally to it. Colonic samples of age-matched controls were also collected. Small pieces (2-3 mm) of the colonic segments for light- and electron microscopic morphometry and post-embedding immunohistochemistry were fixed in 20 g/L formaldehyde and 20 g/L glutaraldehyde solution and embedded in Epon (Electron Microscopy Sciences, Hatfield, PA, United States). Gut segments for molecular studies were cut along the mesentery and pinched flat. After longitudinal cutting, the mucosa and submucosa were removed. Half of the colon samples were immediately frozen in liquid N₂ and later processed for western blot analysis. The other half were incubated overnight at 4 °C in RNA Later (Qiagen, Venlo, The Netherlands) and stored at -80 °C until processing for quantitative real-time PCR (qRT PCR).

Light- and transmission electronmicroscopic morphometry

The Epon blocks were used to prepare semithin (0.7 μ m) sections, which were stained with 10 g/L toluidine blue solution for the light-microscopic study. In the selected area of interest in the semithin cross-sections, all the layers of the gut wall were well oriented. The thicknesses of the LMM and the external circular (CM) and longitudinal (LM) smooth muscle layers were measured at random points with Image J 1.44 (National Institute of Health, Bethesda, MD, United States). The same Epon blocks were used to prepare ultrathin (70 nm) sections and the samples were mounted on nickel grids. Three grids per block were stained with uranyl acetate (Merck, Darmstadt, Germany) and lead citrate (Merck) and were examined and photographed with a Philips CM 10 electronmicroscope equipped with a MEGAVIEW II camera. The width of 15 tight junctions (TJs), *i.e.*, the distance between adjacent enterocytes, was measured at a magnification of $\times 46000$ in the control samples and in the strictures by using the AnalySIS 3.2 program (Soft Imaging System GmbH, Münster, Germany). The distance between SMCs was determined to evaluate the expansion of the ECM within the muscularis externa (ME). Ten montage photographs per intestinal segment were made at a magnification of $\times 10500$ and the distance of SMCs was evaluated in limited-size (2000 nm \times 2000 nm) grids for all images, at the intersection of the grid lines, perpendicularly to the cells and calculated by using the AnalySIS 3.2 program. The mean distance was calculated by using the AnalySIS 3.2 program.

Post-embedding immunohistochemistry

The Epon-embedded tissue blocks used previously for the morphometry also served for the post-embedding immunohistochemistry of caspase 9, as described

earlier^[25]. Briefly, ultrathin sections from each block were sequentially incubated with anti-caspase 9 (Sigma-Aldrich, St. Louis, MO, United States; final dilution 1:50) primary antibodies overnight, followed by protein A-gold-conjugated anti-rabbit (18 nm gold particles, Jackson ImmunoResearch, West Grove, PA, United States; final dilution 1:20) secondary antibodies for 3 h, with extensive washing between. Sections were counterstained with uranyl acetate and lead citrate, and then examined and photographed with a Philips CM10 electronmicroscope equipped with a MEGAVIEW II camera. The numbers of gold particles were counted on digital photographs at a magnification of $\times 25000$ in 10 SMCs and at a magnification of $\times 34000$ in 5 myenteric ganglia (MGs) per colonic segment in each experimental groups with the AnalySIS 3.2 program.

Statistical analysis

Statistical analysis of the histological results was performed by using one-way ANOVA and the Newman-Keuls test with GraphPad Prism 4.0 (GraphPad Software, La Jolla, CA, United States), and a probability $P < 0.05$ was set as the level of significance. The results were expressed as mean \pm SE. The statistical methods of the study were reviewed by Mária Bagyánszki from University of Szeged.

Quantitative real-time polymerase chain reaction

Tissue samples were homogenized in AccuZol (Bioneer, Daejeon, South Korea) directly before qRT PCR. Total RNA was prepared from tissue homogenates as suggested by the manufacturer (Bioneer, Daejeon, Korea). The reverse transcription was achieved by using a High Capacity cDNA Reverse Transcription Kit (Applied Biosystems, Foster City, CA, United States) as described earlier^[24]. qRT PCR was performed in an Exicycler 96 (Bioneer, Daejeon, Korea) in a total volume of 20 μ L containing 10 μ L of FastStart SYBR Green PCR Master Mix, 1 μ L of specific primer (0.5 pmol/ μ L) and 50 ng of cDNA template. The PCR program began with a 15-min initial step at 95 $^{\circ}$ C, followed by 45 cycles of 15 s at 95 $^{\circ}$ C for denaturation, 45 s at 60 $^{\circ}$ C for annealing and 25 s at 72 $^{\circ}$ C for extension. The sequences of primers were derived from NCBI RefSeq Database entry NM_031131.1 for TGF-beta 2 (forward: 5' agtgggcagctttgtctc 3' and reverse: 5' gtgaaagtggcgggatg 3'), NM_013174.2 for TGF-beta 3 (forward: 5' gaagagggccctggacac 3' and reverse: 5' gcgcacacagcagttctc 3'), NM_031055.1 for MMP9 (forward: 5'cctctgcatgaagacgacataa 3' and reverse: 5' ggtcaggtttagagccacga 3') and NM_053819.1 for TIMP1 (forward: 5' cagcaaaaggccttcgtaa 3' and reverse: 5' tggctgaacagggaaacact 3'). Hypoxanthine guanine phosphoribosyltransferase (HPRT) (NCBI RefSeq Database entry: NM_012583.2; forward: 5' gaccggttctgtcatgtcg 3' and reverse 5' acctggttcacatcactaatcac 3') was used as a housekeeping

gene to normalize the expression data. The results were expressed as mean \pm SD.

Western blotting analysis and gelatine zymography

Tissue samples were homogenized in TRIS-mannitol buffer and the total cellular protein was then denatured (mixing and boiling with v/v 20 mmol/L Tris 7-9, 3 mmol/L EDTA, 20 g/L sodium dodecyl sulphate (SDS), 100 g/L mercaptoethanol and 200 g/L glycerol) from each sample as described earlier^[26]. Aliquots of 10 μ g of total cellular protein were electrophoresed by 100 g/L SDS-polyacrilamide gel, and transferred to nitrocellulose membrane (Amersham, Buckinghamshire, United Kingdom). Two hours after blocking (with PBS pH 7.4, 2.5 g/L Tween 20 (v/v) and 50 g/L non-fat dried milk), the membranes were probed with anti-MMP9 mouse monoclonal antibody (Abcam PLC, Cambridge, United Kingdom; final dilution 1:1000) or TIMP1 (H150) rabbit polyclonal antibody (Santa Cruz Biotechnology Inc., Santa Cruz, CA, United States; final dilution 1:1000) for 2 h, and then incubated with horseradish peroxidase-conjugated anti-mouse or anti-rabbit antibody (Santa Cruz Biotechnology Inc., Santa Cruz, CA, United States; final dilution 1:2000) for 1 h at room temperature with extensive PBS-Tween 20 washing between. Immunoreaction was visualized with an Immobilon Western HRP Substrate enhanced chemiluminescence system (Millipore Corporation, Billerica, MA, United States) and scanned with a LI-COR C-DiGit™ Blot Scanner (Li-Cor Corporate, Lincoln, NE, United States).

The activity of MMP9 was determined by gelatine zymography, performed by diluting colonic homogenates in zymogram sample buffer (Bio-Rad, Hercules, CA, United States) and electrophoresing the samples in precast 100 g/L SDS-PAGE containing gelatine (20 mg/mL; Sigma-Aldrich, St. Louis, MO, United States) at 120 V until resolution was achieved. The gels were removed from their casings, gently rinsed in ddH₂O, placed onto a shaker in 1X renaturation buffer (Bio-Rad, Hercules, CA, United States) for 40 min, and then placed in 1X development buffer (Bio-Rad Hercules, CA, United States). With change of the buffer once at 20 min, the gels were next incubated at 37 $^{\circ}$ C for 20 h and stained with Coomassie Blue (Bio-Rad, Hercules, CA, United States) for 40 min before being destained in water for 1 h and scanned with a LI-COR C-DiGit™ Blot Scanner.

RESULTS

General observations

Despite the severity of the acute intestinal inflammation of the TNBS-treated rats, the mortality was negligible: only 2 rats died throughout the 120-d experimental period. By 1 d following the TNBS treatment, all the animals had developed symptoms such as weakness, weight loss and bloody diarrhoea. However, by 7 or 8



Figure 1 Representative micrographs from the distal colon of rats with chronic colitis 90 d after the first (A), second (B) or third (C) treatment with 2,4,6-trinitrobenzenesulfonic acid. The frequency and size of the strictures (arrows) increased in the time and with the number of 2,4,6-trinitrobenzenesulfonic acid (TNBS) administrations.

d after TNBS administrations, all the visible symptoms accompanied by acute inflammation had resolved. By day 60 following TNBS treatments, all the rats that had previously been exposed to acute colitis had regained their initial body weight and strictures had appeared in each TNBS-treated group. We, therefore, investigated the structural and molecular characteristics of the strictured gut wall from this timepoint on. Whereas the numbers and sizes of the strictures increased in time and with the number of TNBS treatments, they always developed within the previously inflamed colonic areas (Figure 1) and, once they had appeared, their structure and molecular characteristics did not differ. To avoid repetitions therefore, representative results will be presented here, obtained after the processing of tissue samples collected exclusively after the third TNBS administration.

Light microscopy

Representative images of toluidine blue-stained semithin sections of colon where the thickness of the ME was measured are shown in Figure 2. Such colonic sections were collected for measurements on days 90 and 120 following TNBS administrations and also from age-matched controls. The strictured colonic regions displayed normal mucosal architecture and clearly defined, yet thickened muscle layers (not shown). Morphometric analyses revealed the approximately 2-fold thickening of the LMM and layers of the ME in the strictured region relative to the control samples on 90 d. While further significant thickening of the ME was measured beyond day 90 after TNBS administrations, the thickness of the LMM at later than 90 d was similar to that in the controls (Figure 2).

Transmission electronmicroscopy

Transmission electronmicroscopic examination of the colonic epithelium in the strictured region on days 90 and 120 after TNBS administrations showed that the apical surface of the enterocytes with intact brush-border and closed TJs was similar to that in the controls (Figure 3). The width of the TJs between adjacent enterocytes was evaluated morphometrically and was always found to be less than 3 nm (data not shown). However, autophagosome-like double-membrane vesicles of different sizes were frequently seen within the enterocytes (Figure 3).

Because of the excess accumulation of ECM elements in the strictured colonic regions, the SMCs

had moved away from each other significantly by day 90 after TNBS administrations, and by 120 d there was more than 2-fold increase in the distance between adjacent SMCs as compared with the controls (Figure 4). Because of the ECM deposition, the SMCs also moved away from the MGs (Figure 4). By day 120 post-TNBS treatments, swollen and empty confluent vacuoles and autophagosomes were frequently seen in the SMCs and also in their close environment, together with different cell organelles in the strictured colonic areas (Figure 4). The vast majority of the axons appeared normal, but necrotic axons were seen rarely in the MGs (Figure 4). Quantitative post-embedding immunohistochemistry in the strictured areas revealed a progressive increase in the number of gold particles indicating caspase 9 antigen in the SMCs and MGs relative to the control samples (Figure 5). The caspase 9-labelling gold particles in the MGs were mainly associated with the mitochondria (Figure 5), the ultrastructure of which was well preserved even 120 d after TNBS treatments.

Quantitative changes in TGF-beta, MMP9 and TIMP1 mRNA and protein expression

On day 90, the TGF-beta 2 mRNA was up-regulated, while the TGF-beta 3 mRNA was down-regulated in the strictured gut wall and also in the colonic segments adjacent proximally and distally to the strictures as compared with the controls. The TGF-beta 2 mRNA expression progressively increased, while the TGF-beta 3 mRNA expression further decreased by day 120 in all three segments (Figure 6A).

A marked overexpression of MMP9 mRNA was detected in all the colonic segments examined on days 90 and 120 after TNBS treatments (Figure 6B). At the same timepoints, the TIMP1 mRNA expression was up-regulated in the colonic segments adjacent proximally and distally to the strictures, but was down-regulated in the strictures themselves (Figure 6B). MMP9 and TIMP1 expression was also evaluated at the protein levels. Although a high amount of MMP9 protein was demonstrated in the tissue samples from the control rats, the progressive increase in the amount of MMP9 protein in the strictures was obvious between days 90 and 120 (Figure 6C). Gelatine zymography demonstrated that an active form of MMP9 protein rather than pro-MMP was expressed (Figure 6C). While the amount of TIMP1 protein also decreased acutely between days 90 and 120 in the control samples, it was

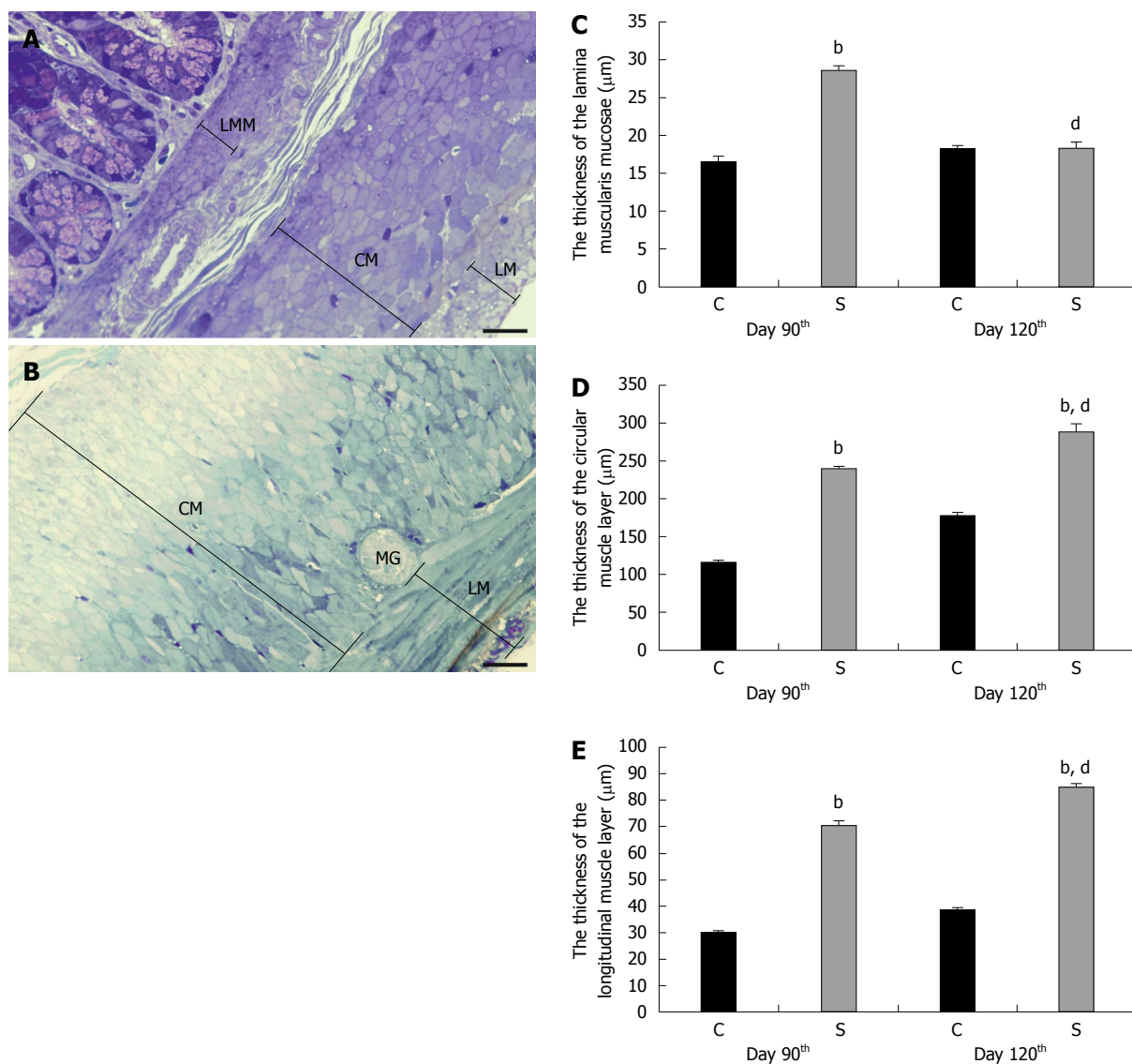


Figure 2 Thickness of the smooth muscle layers in the colon of control animals and in rats treated three times with 2,4,6-trinitrobenzenesulfonic acid. A: Representative light micrographs of a toluidine blue-stained semithin section from the colon of a control rat; B: TNBS-treated rat on day 120 of the experimental period. Bar: 25 μm . Significant thickening of the LMM (C), CM (D) and LM (E) was demonstrated in the strictured gut wall of the TNBS-treated rats (S) relative to the controls (C) on day 90. Whereas a further significant thickening was measured in the CM and LM on day 120, the thickness of the LMM was similar to that in the controls at this timepoint. Data are expressed as mean \pm SE. ^a $P < 0.001$ TNBS-treated groups vs age-matched controls; ^b $P < 0.001$ 2,4,6-trinitrobenzenesulfonic acid (TNBS)-treated group on day 90 vs TNBS-treated group on day 120. LMM: Lamina muscularis mucosae; CM: Circular muscle layer; LM: Longitudinal muscle layer; MG: Myenteric ganglion.

practically undetectable in the strictures (Figure 6C).

DISCUSSION

We recently reported on a rat model in which all-leviated inflammatory damage in association with the persistent up-regulation of HO-1 were salient features in the acute phase of intestinal inflammation induced by repeated TNBS administrations^[24]. The same model was used in the present work to investigate the structural and molecular events leading to the formation of a strictured gut wall. Concerning the long-term consequences of the acute inflammation in this model, all the visible symptoms had resolved by day 60 after TNBS administration, the body weight of the

treated rats was similar to that of the age-matched controls, and intestinal strictures developed in all of the rats that had previously displayed intestinal inflammation. These findings accord well with the clinical observations that mucosal healing and clinical remission alone cannot be treatment endpoints in CD, because this does not prevent later stricturing^[27,28]. The increases in size and frequency of the strictures observed here after 60 d provide experimental evidence in favour of the view that strictures, once present, gradually progress and, once fibrosis develops, it cannot be reversed^[29].

Aligned thickening of all the muscle layers in the strictured gut wall until up to day 90 after TNBS administrations was characteristic. Whereas the thic-

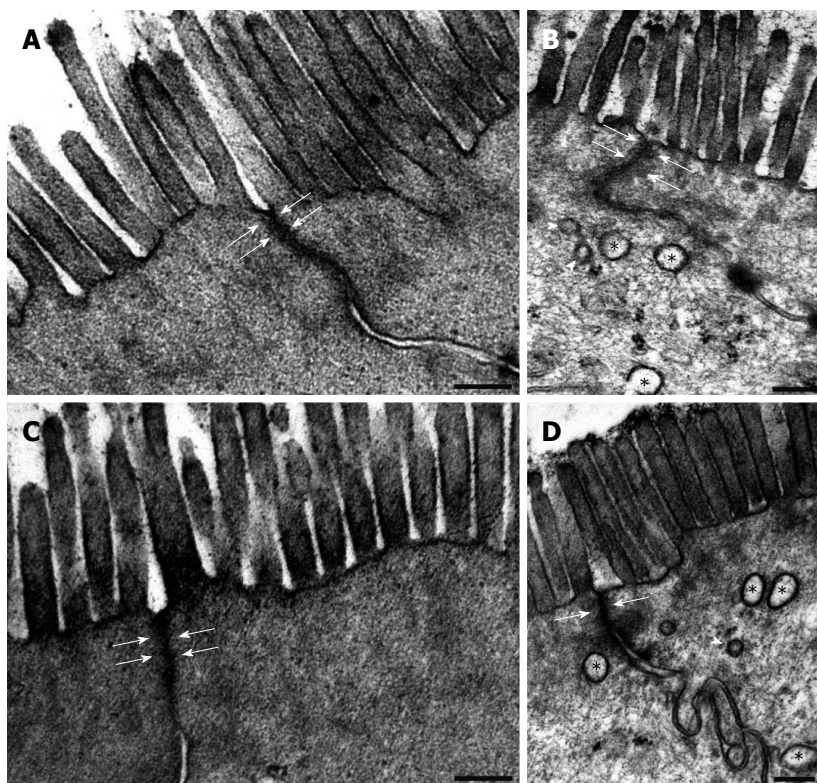


Figure 3 Representative electron micrographs of two neighbouring enterocytes from the colon of control animals (A, C) and in rats treated three times with 2,4,6-trinitrobenzenesulfonic acid. On days 90 (B) and 120 (D) following the third 2,4,6-trinitrobenzenesulfonic acid (TNBS) administration, both the microvillar surface and the width of the apical intercellular tight junctions (arrows) of the enterocytes in the strictured regions were similar to those in the age-matched controls (A on day 90 and C on day 120). However, autophagosomes (asterisks) and lysosomes (arrowheads) were commonly observed within the epithelial cells of the strictured gut wall. Bars: 200 nm.

kening of the ME progressed further and became a decisive element of the strictured gut wall, the thickness of the LMM did not change after day 90, and did not differ from that in the controls by the end of the experimental period. Since the LMM is most involved in maintaining the mucosal integrity^[30], we suppose that the earlier cessation of excess ECM deposition in the LMM is a consequence of the differential regulation of inflammation-related events here through cytokines derived from the epithelium^[31,32].

At 90 and 120 d following TNBS administrations, transmission electron microscopy showed that the structures of the epithelium necessary to maintain the barrier functions were intact. However, the frequent presence of double-membrane autophagosomes indicated high levels of intracellular stressors in the previously affected epithelium. It has been well documented that induction of autophagy is a determining factor for the maintenance of cellular homeostasis in chronic colitis^[33,34]. The importance of autophagy in the pathogenesis of chronic intestinal inflammation has also been demonstrated by genome-wide association studies which identified a link between the genes involved in autophagy regulation and IBDs^[35,36].

While the rapid and widespread loss of myenteric neurons was a characteristic feature of the onset of

acute inflammation^[24], the precise timing of the cellular events in the chronic phase leading to the intestinal stricturing here showed that the SMCs in the ME were affected first in these processes. Since the excess deposition of ECM in the ME was sustained throughout the experimental period, the SMCs progressively moved away from each other and also from the MGs, leading eventually to deficient innervation and severe cellular damage. After day 60 following TNBS treatments, the appearance of autophagosomes, the leakage of cellular contents and the increasing number of gold particles labelling caspase 9 expression indicated that all three types of cell death mechanisms had already progressed in the SMCs by day 90 when necrotic axons were only rarely seen in the MGs. As the pathological environment became more extensive with time, by day 120 after TNBS administration locally severe neuronal injury also occurred in the strictured tissue as a significant sign of chronic inflammation, similarly as described in other models^[23,37]. As regards the timing of the events, we presume suppose that the neuronal injury is a consequence and not the cause of the stricturing processes.

Evidence from both animal models^[38,39] and human studies^[18,40,41] has suggested that the up-regulation of TGF-beta 2 and of MMP9 may be considered to be biomarkers in the post-inflammatory tissue

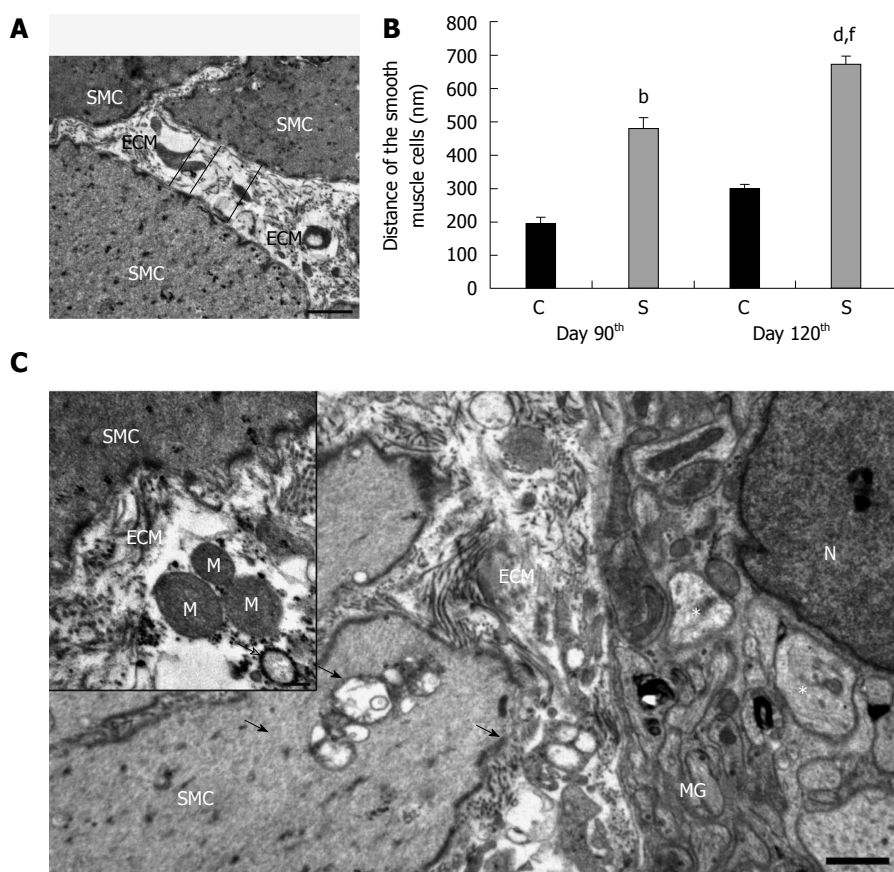


Figure 4 Ultrastructural alterations within the colon of control animals and in rats treated three times with 2,4,6-trinitrobenzenesulfonic acid. Excess deposition of extracellular matrix (ECM) was observed within the smooth muscle layers in the ultrathin sections derived from the strictured region (A); Electronmicroscopic morphometry revealed that the distance between adjacent smooth muscle cells (SMCs) was significant larger in the strictured gut wall of the 2,4,6-trinitrobenzenesulfonic acid (TNBS)-treated rats (S) as compared with the gut wall of the control rats (C) on day 90 (B); A further significant increase in the mean separation distance of the SMCs was recorded on day 120 post-TNBS treatment (B). Data are expressed as mean \pm SE. ^b $P < 0.01$, ^a $P < 0.001$ TNBS-treated groups vs age-matched controls; ^f $P < 0.001$ TNBS-treated group on the day 90 vs TNBS-treated group on day 120. Representative electron micrograph of the strictured colonic area 120 d after the third TNBS administration (C). Because of ECM accumulation, the SMCs also moved away from the myenteric ganglia (MGs). Swollen and empty confluent vacuoles of different sizes (arrows) were frequently seen in the SMCs and also in their close environment. Rupture of the plasma membrane and subsequent leakage of the cell organelles into the microenvironment, e.g., the mitochondria (M) and autophagosomes (hollow arrow), were frequently seen in the intercellular spaces (insert). However, the vast majority of the axons appeared normal; necrotic axons were rarely seen in the MGs (asterisks). N: Nucleus. Bars: 1 μ m and 200 nm (insert).

remodelling leading to stricturing in CD. The mRNA expression profile of the TGF-beta isoforms, the up-regulation of TGF-beta 2 and the down-regulation of TGF beta 3 in the colonic segments examined in our model accorded well with the distinctive expressional profile of the secreted TGF-beta isoforms in human CD primary intestinal myofibroblasts^[41]. The spreading of this characteristic expression pattern both proximally and distally to the strictures indicated the bidirectional diffusion of the disease along the colon in our model. We also detected progressive up-regulation of MMP9 mRNA in all three colonic segments, suggesting again the proximally and distally directed diffusion of the pathological environment. However, the MMP9 up-regulation in the strictured gut wall was coupled with the down-regulation of TIMP1, and an increased amount of active MMP9, but no TIMP1 protein was detected here, indicating a stricture-specific off-balance in the production of proteases and their inhibitors. This expression pattern is very reminiscent

of that which develops in the fistulae in approximately one-third of patients with CD^[42]. The apparent differences in expression profiles between our study and the literature data in tissue samples prepared from the control guts could be explained by the different methodological approaches. The novelty of our studies was that we prepared tissue homogenates for molecular studies not from the mucosa overlying the strictures, but exclusively from the ME, where the background events of the chronic inflammation leading to stricture formation actually occurred.

In conclusion, The structural and molecular events leading to stricturing as a long-term consequence of acute intestinal inflammation that were demonstrated earlier in animal models and in human studies also characterized the stricture formation induced in our rat model by repeated TNBS administrations. Since the exact timing of the stricturing processes was possible in this model, we reached the conclusion that, in contrast with the general view, the ME, and not the

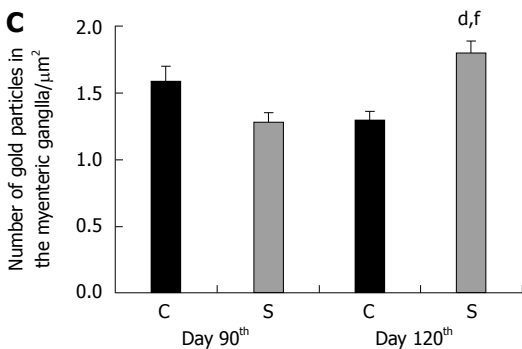
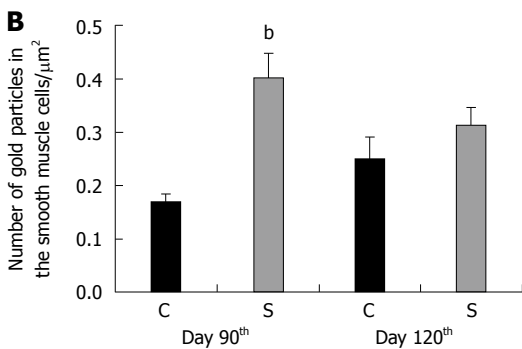


Figure 5 Post-embedding immunogold labelling for caspase 9 in the smooth muscle cells and myenteric ganglia in the colon of control animals and in rats treated three times with 2,4,6-trinitrobenzenesulfonic acid. Representative electron micrograph of a myenteric ganglion (MG) from the strictured gut wall (S) 120 d after the third 2,4,6-trinitrobenzenesulfonic acid (TNBS) administration (A). The 18 nm gold particles labelling caspase 9 immunoreactivity (arrows) were mainly associated with mitochondria (M). Bar: 200 nm. The number of gold particles in the S was increased significantly in the smooth muscle cells on day 90 (B) and also in the MGs on day 120 (C) as compared with the gut wall in the control rats (C). Data are expressed as mean ± SE. ^b*P* < 0.01, ^{d,f}*P* < 0.001 TNBS-treated groups vs age-matched controls; ^f*P* < 0.01 TNBS-treated group on the day 90 vs TNBS-treated group on day 120.

epithelial barrier or the MGs, was the primary target of the events leading to stricture formation. Moreover, this TNBS-induced rat model has provided the first experimental demonstration of the molecular diffusion of the disease both proximally and distally along the gut wall. The off-balance in MMP9/TIMP1 expression profile found strictly within the border of the strictures may well allow use of this model to investigate the molecular mechanisms leading to fistulated CD.

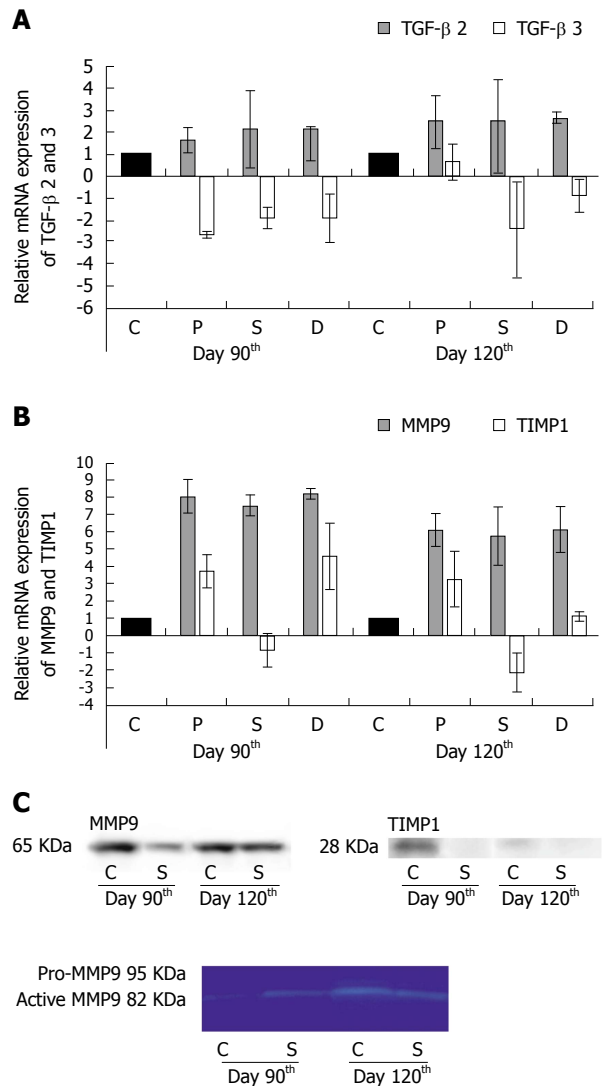


Figure 6 Relative mRNA and protein expression of transforming growth factor-beta 2 and 3, matrix metalloproteinase 9 and tissue inhibitor of metalloproteinases 1 in the colon of control animals and in rats treated three times with 2,4,6-trinitrobenzenesulfonic acid. TGF-beta 2 was up-regulated in the strictured region (S) and also in the adjacent proximal (P) and distal (D) segments of the colon as compared with the controls (C) on day 90 and day 120 (A). TGF-beta 3 gene repression was detected both 90 and 120 d after the third TNBS treatment in each colonic segment (A). The marked overexpression of MMP9 mRNA was confirmed in each colonic segment in the chronic phase of the inflammation (B). TIMP1 mRNA expression was detected in the P and D colon segments at both timepoints examined, but in the S the gene was down-regulated (B). Data are expressed as mean ± SD. 90 d after the third TNBS treatment, a decreased MMP9 protein level was detected in the S relative to the C (C, upper). Nevertheless, on day 120 the MMP9 protein expression was similar to that in the C. The activity of MMP9 was determined by gelatine zymography (C, lower). An active form of the MMP9 protein rather than pro-MMP9 was expressed in the C and S segments at both timepoints examined. Well-detectable amounts of TIMP1 protein were revealed only in the control samples from day 90 (C, right side).

COMMENTS

Background

Intestinal strictures are characteristic complications of Crohn's disease (CD) affecting more than one third of all patients. Its can lead to partial or total

intestinal obstruction with potentially life-threatening consequences. Although the treatment of the chronic complications of CD is a serious medical problem, the pathogenesis, factors, and cell types involved in stricture formation are largely unknown.

Research frontiers

Despite of the huge amount of animal models and human studies, the structural and molecular events leading to stricturing as a long-term consequence of acute intestinal inflammation are still not clear until today. Besides, the ultrastructure of the intestinal strictures is still unknown.

Innovations and breakthroughs

This TNBS-induced rat model has provided the first experimental demonstration of that, in contrast with the general view, the muscularis externa, and not the epithelial barrier or the myenteric ganglia, was the primary target of the events leading to stricture formation.

Applications

The authors hypothesize from the results derived our rat model with chronic colitis and very low mortality that the experimentally provoked recurrent relapsing inflammations characteristic to CD can provoke the recrudescence of the strictures post-surgically despite of the complete mucosal healing and restoring myenteric neuronal injury.

Terminology

The authors described earlier that experimentally provoked repetitive relapsing inflammations develop preconditioning effect by speeding up mucosal healing and restoring myenteric neuronal injury.

Peer-review

This is a well-written manuscript with carefully designed and described experiments. The observations are interesting and certainly add to our knowledge in the inflammation-induced fibrosis in the large intestine.

REFERENCES

- Chang CW, Wong JM, Tung CC, Shih IL, Wang HY, Wei SC. Intestinal stricture in Crohn's disease. *Intest Res* 2015; **13**: 19-26 [PMID: 25691840 DOI: 10.5217/ir.2015.13.1.19]
- Neurath MF, Travis SP. Mucosal healing in inflammatory bowel diseases: a systematic review. *Gut* 2012; **61**: 1619-1635 [PMID: 22842618 DOI: 10.1136/gutjnl-2012-302830]
- Tan M, Ong JP, Teo EK. Achieving deep remission in Crohn's disease: treating beyond symptoms. *Ann Acad Med Singapore* 2014; **43**: 200-202 [PMID: 24833070]
- Orlando A, Guglielmi FW, Cottone M, Orlando E, Romano C, Sinagra E. Clinical implications of mucosal healing in the management of patients with inflammatory bowel disease. *Dig Liver Dis* 2013; **45**: 986-991 [PMID: 23993738 DOI: 10.1016/j.dld.2013.07.005]
- Burke JP, Mulsow JJ, O'Keane C, Docherty NG, Watson RW, O'Connell PR. Fibrogenesis in Crohn's disease. *Am J Gastroenterol* 2007; **102**: 439-448 [PMID: 17156147 DOI: 10.1111/j.1572-0241.2006.01010.x]
- Rieder F, Fiocchi C. Mechanisms of tissue remodeling in inflammatory bowel disease. *Dig Dis* 2013; **31**: 186-193 [PMID: 24030223 DOI: 10.1159/000353364]
- Rieder F, Brenmoehl J, Leeb S, Schölmerich J, Rogler G. Wound healing and fibrosis in intestinal disease. *Gut* 2007; **56**: 130-139 [PMID: 17172588 DOI: 10.1136/gut.2006.090456]
- Hills CE, Squires PE. TGF-beta1-induced epithelial-to-mesenchymal transition and therapeutic intervention in diabetic nephropathy. *Am J Nephrol* 2010; **31**: 68-74 [PMID: 19887790 DOI: 10.1159/000256659]
- Shah M, Foreman DM, Ferguson MW. Neutralising antibody to TGF-beta 1,2 reduces cutaneous scarring in adult rodents. *J Cell Sci* 1994; **107** (Pt 5): 1137-1157 [PMID: 7929624]
- Shah M, Foreman DM, Ferguson MW. Neutralisation of TGF-beta 1 and TGF-beta 2 or exogenous addition of TGF-beta 3 to cutaneous rat wounds reduces scarring. *J Cell Sci* 1995; **108** (Pt 3): 985-1002 [PMID: 7542672]
- Wang B, Koh P, Winbanks C, Coughlan MT, McClelland A, Watson A, Jandeleit-Dahm K, Burns WC, Thomas MC, Cooper ME, Kantharidis P. miR-200a Prevents renal fibrogenesis through repression of TGF-beta2 expression. *Diabetes* 2011; **60**: 280-287 [PMID: 20952520 DOI: 10.2337/db10-0892]
- Woessner JF. Matrix metalloproteinases and their inhibitors in connective tissue remodeling. *FASEB J* 1991; **5**: 2145-2154 [PMID: 1850705]
- Birkedal-Hansen H, Moore WG, Bodden MK, Windsor LJ, Birkedal-Hansen B, DeCarlo A, Engler JA. Matrix metalloproteinases: a review. *Crit Rev Oral Biol Med* 1993; **4**: 197-250 [PMID: 8435466]
- Nelson AR, Fingleton B, Rothenberg ML, Matrisian LM. Matrix metalloproteinases: biologic activity and clinical implications. *J Clin Oncol* 2000; **18**: 1135-1149 [PMID: 10694567]
- Overall CM. Dilating the degradome: matrix metalloproteinase 2 (MMP-2) cuts to the heart of the matter. *Biochem J* 2004; **383**: e5-e7 [PMID: 15508185 DOI: 10.1042/BJ20041433]
- Parks WC, Wilson CL, López-Boado YS. Matrix metalloproteinases as modulators of inflammation and innate immunity. *Nat Rev Immunol* 2004; **4**: 617-629 [PMID: 15286728 DOI: 10.1038/nri1418]
- Overall CM, Kleinfeld O. Towards third generation matrix metalloproteinase inhibitors for cancer therapy. *Br J Cancer* 2006; **94**: 941-946 [PMID: 16538215 DOI: 10.1038/sj.bjc.6603043]
- Kofla-Dlubacz A, Matusiewicz M, Krzystek-Korpaczka M, Iwanczak B. Correlation of MMP-3 and MMP-9 with Crohn's disease activity in children. *Dig Dis Sci* 2012; **57**: 706-712 [PMID: 21997756 DOI: 10.1007/s10620-011-1936-z]
- Lourensen S, Wells RW, Blennerhassett MG. Differential responses of intrinsic and extrinsic innervation of smooth muscle cells in rat colitis. *Exp Neurol* 2005; **195**: 497-507 [PMID: 16098965 DOI: 10.1016/j.expneurol.2005.06.012]
- Skobowiat C, Gonkowski S, Calka J. Phenotyping of sympathetic chain ganglia (SChG) neurons in porcine colitis. *J Vet Med Sci* 2010; **72**: 1269-1274 [PMID: 20460841 DOI: 10.1292/jvms.10-0081]
- Skobowiat C, Calka J, Majewski M. Axotomy induced changes in neuronal plasticity of sympathetic chain ganglia (SChG) neurons supplying descending colon in the pig. *Exp Mol Pathol* 2011; **90**: 13-18 [PMID: 21110956 DOI: 10.1016/j.yexmp.2010.11.004]
- Skobowiat C. Contribution of Neuropeptides and Neurotransmitters in colitis. *J Veterinar Sci Technol* 2012; **3**: 1 [DOI: 10.4172/2157-7579.S5-001]
- Marlow SL, Blennerhassett MG. Deficient innervation characterizes intestinal strictures in a rat model of colitis. *Exp Mol Pathol* 2006; **80**: 54-66 [PMID: 15990093 DOI: 10.1016/j.yexmp.2005.04.006]
- Talapka P, Nagy LI, Pál A, Poles MZ, Berkó A, Bagyánszki M, Puskás LG, Fekete É, Bódi N. Alleviated mucosal and neuronal damage in a rat model of Crohn's disease. *World J Gastroenterol* 2014; **20**: 16690-16697 [PMID: 25469038 DOI: 10.3748/wjg.v20.i44.16690]
- Bódi N, Talapka P, Poles MZ, Hermes E, Jancsó Z, Katarova Z, Izbéki F, Wittmann T, Fekete É, Bagyánszki M. Gut region-specific diabetic damage to the capillary endothelium adjacent to the myenteric plexus. *Microcirculation* 2012; **19**: 316-326 [PMID: 22296580 DOI: 10.1111/j.1549-8719.2012.00164.x]
- Horváth K, Varga C, Berkó A, Pósa A, László F, Whittle BJ. The involvement of heme oxygenase-1 activity in the therapeutic actions of 5-aminosalicylic acid in rat colitis. *Eur J Pharmacol* 2008; **581**: 315-323 [PMID: 18215658 DOI: 10.1016/j.ejphar.2007.12.004]
- Osterman MT, Haynes K, Delzell E, Zhang J, Bewtra M, Brensinger C, Chen L, Xie F, Curtis JR, Lewis JD. Comparative effectiveness of infliximab and adalimumab for Crohn's disease. *Clin Gastroenterol Hepatol* 2014; **12**: 811-817.e3 [PMID: 23811254 DOI: 10.1016/j.cgh.2013.06.010]

- 28 **Neurath MF.** New targets for mucosal healing and therapy in inflammatory bowel diseases. *Mucosal Immunol* 2014; **7**: 6-19 [PMID: 24084775 DOI: 10.1038/mi.2013.73]
- 29 **Rieder F, Zimmermann EM, Remzi FH, Sandborn WJ.** Crohn's disease complicated by strictures: a systematic review. *Gut* 2013; **62**: 1072-1084 [PMID: 23626373 DOI: 10.1136/gutjnl-2012-304353]
- 30 **Kagnoff MF.** The intestinal epithelium is an integral component of a communications network. *J Clin Invest* 2014; **124**: 2841-2843 [PMID: 24983425 DOI: 10.1172/JCI175225]
- 31 **Yang SK, Eckmann L, Panja A, Kagnoff MF.** Differential and regulated expression of C-X-C, C-C, and C-chemokines by human colon epithelial cells. *Gastroenterology* 1997; **113**: 1214-1223 [PMID: 9322516 DOI: 10.1053/gast.1997.v113.pm9322516]
- 32 **Sansonetti PJ, Arondel J, Huerre M, Harada A, Matsushima K.** Interleukin-8 controls bacterial transepithelial translocation at the cost of epithelial destruction in experimental shigellosis. *Infect Immun* 1999; **67**: 1471-1480 [PMID: 10024597]
- 33 **Ogata M, Hino S, Saito A, Morikawa K, Kondo S, Kanemoto S, Murakami T, Taniguchi M, Tani I, Yoshinaga K, Shiosaka S, Hammarback JA, Urano F, Imaizumi K.** Autophagy is activated for cell survival after endoplasmic reticulum stress. *Mol Cell Biol* 2006; **26**: 9220-9231 [PMID: 17030611 DOI: 10.1128/MCB.01453-06]
- 34 **Randall-Demillo S, Chieppa M, Eri R.** Intestinal epithelium and autophagy: partners in gut homeostasis. *Front Immunol* 2013; **4**: 301 [PMID: 24137160 DOI: 10.3389/fimmu.2013.00301]
- 35 **Hampe J, Franke A, Rosenstiel P, Till A, Teuber M, Huse K, Albrecht M, Mayr G, De La Vega FM, Briggs J, Günther S, Prescott NJ, Onnie CM, Häsler R, Sipos B, Fölsch UR, Lengauer T, Platzer M, Mathew CG, Krawczak M, Schreiber S.** A genome-wide association scan of nonsynonymous SNPs identifies a susceptibility variant for Crohn disease in ATG16L1. *Nat Genet* 2007; **39**: 207-211 [PMID: 17200669 DOI: 10.1038/ng1954]
- 36 **Franke A, McGovern DP, Barrett JC, Wang K, Radford-Smith GL, Ahmad T, Lees CW, Balschun T, Lee J, Roberts R, Anderson CA, Bis JC, Bumpstead S, Ellinghaus D, Festen EM, Georges M, Green T, Haritunians T, Jostins L, Latiano A, Mathew CG, Montgomery GW, Prescott NJ, Raychaudhuri S, Rotter JI, Schumm P, Sharma Y, Simms LA, Taylor KD, Whiteman D, Wijmenga C, Baldassano RN, Barclay M, Bayless TM, Brand S, Büning C, Cohen A, Colombel JF, Cottone M, Stronati L, Denson T, De Vos M, D'Inca R, Dubinsky M, Edwards C, Florin T, Franchimont D, Gearry R, Glas J, Van Gossum A, Guthery SL, Halfvarson J, Verspaget HW, Hugot JP, Karban A, Laukens D, Lawrance I, Lemann M, Levine A, Libioulle C, Louis E, Mowat C, Newman W, Panés J, Phillips A, Proctor DD, Regueiro M, Russell R, Rutgeerts P, Sanderson J, Sans M, Seibold F, Steinhart AH, Stokkers PC, Torkvist L, Kullak-Ublick G, Wilson D, Walters T, Targan SR, Brant SR, Rioux JD, D'Amato M, Weersma RK, Kugathasan S, Griffiths AM, Mansfield JC, Vermeire S, Duerr RH, Silverberg MS, Satsangi J, Schreiber S, Cho JH, Annese V, Hakonarson H, Daly MJ, Parkes M.** Genome-wide meta-analysis increases to 71 the number of confirmed Crohn's disease susceptibility loci. *Nat Genet* 2010; **42**: 1118-1125 [PMID: 21102463 DOI: 10.1038/ng.717]
- 37 **Lakhan SE, Kirchgessner A.** Neuroinflammation in inflammatory bowel disease. *J Neuroinflammation* 2010; **7**: 37 [PMID: 20615234 DOI: 10.1186/1742-2094-7-37]
- 38 **Medina C, Videla S, Radomski A, Radomski MW, Antolín M, Guarner F, Vilaseca J, Salas A, Malagelada JR.** Increased activity and expression of matrix metalloproteinase-9 in a rat model of distal colitis. *Am J Physiol Gastrointest Liver Physiol* 2003; **284**: G116-G122 [PMID: 12488238]
- 39 **Medina C, Santana A, Paz MC, Díaz-Gonzalez F, Farre E, Salas A, Radomski MW, Quintero E.** Matrix metalloproteinase-9 modulates intestinal injury in rats with transmural colitis. *J Leukoc Biol* 2006; **79**: 954-962 [PMID: 16478919 DOI: 10.1189/jlb.1005544]
- 40 **Baugh MD, Perry MJ, Hollander AP, Davies DR, Cross SS, Lobo AJ, Taylor CJ, Evans GS.** Matrix metalloproteinase levels are elevated in inflammatory bowel disease. *Gastroenterology* 1999; **117**: 814-822 [PMID: 10500063 DOI: 10.1016/S0016-5085(99)70339-2]
- 41 **McKaig BC, Hughes K, Tighe PJ, Mahida YR.** Differential expression of TGF-beta isoforms by normal and inflammatory bowel disease intestinal myofibroblasts. *Am J Physiol Cell Physiol* 2002; **282**: C172-C182 [PMID: 11742810 DOI: 10.1152/ajpcell.00048.2001]
- 42 **Kirkegaard T, Hansen A, Bruun E, Brynskov J.** Expression and localisation of matrix metalloproteinases and their natural inhibitors in fistulae of patients with Crohn's disease. *Gut* 2004; **53**: 701-709 [PMID: 15082589 DOI: 10.1136/gut.2003.017442]

P- Reviewer: Bayraktar Y, Kuo SM, Nakajima H, Ohkohchi N
S- Editor: Qi Y L- Editor: A E- Editor: Wang CH





Published by **Baishideng Publishing Group Inc**

8226 Regency Drive, Pleasanton, CA 94588, USA

Telephone: +1-925-223-8242

Fax: +1-925-223-8243

E-mail: bpgooffice@wjgnet.com

Help Desk: <http://www.wjgnet.com/esps/helpdesk.aspx>

<http://www.wjgnet.com>



ISSN 1007-9327



9 771007 932045